

Snowmelt runoff conceptualization based on tracer and satellite data

JAROSLAV MARTINEC

Alteinstrasse 10, CH-7270 Davos-Platz, Switzerland

ALBERT RANGO

USDA Hydrology Laboratory, BARC-West, Building 007, Room 104, Beltsville, Maryland 20705, USA

e-mail: alrango@hydrolab.arsusda.gov

Abstract As a result of thermonuclear test explosions in the atmosphere, tritium concentrations in precipitation in the sixties and seventies varied strongly from year to year as well as in the winter and summer half years. This paper illustrates how the contrasting tritium concentration in snow and in groundwater was used to develop a snowmelt runoff model (SRM). A new insight into the runoff mechanism and the role of the recession flow provided a concept of transforming the snowmelt into river flow on a daily basis. The adopted deterministic approach, without calibration of parameters, requires snow cover monitoring by satellites. While tritium tracing contributed to the model design, remote sensing enables the SRM model to be used around the world.

INTRODUCTION

Tritium ^3H , the radioactive isotope of hydrogen, emerged as a tracer following thermonuclear test explosions in the atmosphere in the period 1952–1963. The naturally produced tritium by cosmic rays in precipitation amounts to 5–15 tritium units (1 TU = one tritium atom per 10^{18} hydrogen atoms). The thermonuclear explosions injected large amounts of tritium into the atmosphere so that concentrations increased to several thousands TU in the summer of 1963 in the northern hemisphere.

The exchange of information in the scope of the International Hydrological Decade (1965–1974) enabled the International Atomic Energy Agency (IAEA) in Vienna to initiate a joint project in order to exploit this situation (Dinçer *et al.*, 1970). The labelling of precipitation by tritium revealed a major role of groundwater in the runoff generation. This knowledge enabled a relatively simple input–output transformation to be developed. SRM, as a non-calibration model, requires periodical snow cover mapping in mountain basins. With advances in remote sensing (Rango & Itten, 1976), satellite snow cover information rapidly became available so that the model (SRM) was and is widely used around the world (Martinec *et al.*, 1998).

SNOWMELT RUNOFF IN REPRESENTATIVE BASINS

A simple runoff concept developed in the basin Modry Dul takes advantage of the typical daily fluctuations of snowmelt runoff resulting from the daily cycle of

temperature and solar radiation:

$$R_n = c \cdot M(1 - k) + R_{n-1} \cdot k \quad (1)$$

where:

R_n = daily runoff (cm),

M = daily snowmelt (cm),

c = runoff coefficient expressing losses,

k = recession coefficient,

$n, n - 1$ refer to the sequence of days.

The recession coefficient $k = R_m/R_{m-1}$ (where $m, m - 1$ refer to a recession period without snowmelt or rainfall) thus determines which part of the daily snowmelt appears in the runoff within 24 h and which part follows as a recession flow. Even with this simple formula, it was possible to simulate runoff (Dinçer *et al.*, 1970). It appeared to be necessary, however, to adjust the recession coefficient in relation to the current runoff instead of using a constant value as is the case in traditional recession formulae. For daily runoff depths exceeding 12.5 mm, $k = 0.5$ was used; for runoff depths from 5.0 to 12.5 mm, a value of 0.75 was used; and for runoff depths less than 5.0 mm, $k = 0.9$ or even $k = 0.95$ was used. The tritium study enabled this tentative procedure to be replaced by a mathematical formulation as will be explained in the next section.

It was also necessary to take into account the shrinking snow covered area towards the end of the snowmelt season. Because the small basin Modry Dul (Czech Republic, 2.65 km², 1000–1560 m a.s.l.) could be observed in its entirety from one overlook point, the snow coverage was evaluated by ground-based terrestrial observation. This method was not possible in the larger alpine basin Dischma (Switzerland, 43.3 km², 1668–3146 m a.s.l.). Here the snow covered areas were at first evaluated from aerial photographs which had to be rectified to orthophotos, at a considerable cost. In view of the large elevation range, it was necessary to divide the basin into three elevation zones and to compute the snowmelt in each elevation zone separately, with the use of the respective snow covered areas. Soon it became clear that this expensive and time-consuming procedure was not practicable for operational snowmelt runoff computations outside a research project. Advances in remote sensing (Rango & Itten, 1976) and the ever-improving methods of satellite snow cover mapping (Baumgartner, 1987; Seidel *et al.*, 1996; Ehrler *et al.*, 1997) solved this problem, as will be explained in a later section.

RUNOFF COMPONENTS TRACED BY TRITIUM

The variations of tritium concentrations in precipitation in central Europe in the period 1954–1979 are shown in Fig. 1. As a result of the timing and strength of thermonuclear explosions, variations occurred in the course of years. In addition, differences between the winter and summer values reflected the intensity of mixing between the stratosphere and troposphere. Consequently, an extensive sampling of precipitation, snow cover, winter baseflow (originating from groundwater reserves) and snowmelt runoff in the basins Modry Dul and Dischma (Dinçer *et al.*, 1970; Martinec *et al.*, 1982a) revealed significantly different tritium concentrations. The participation of

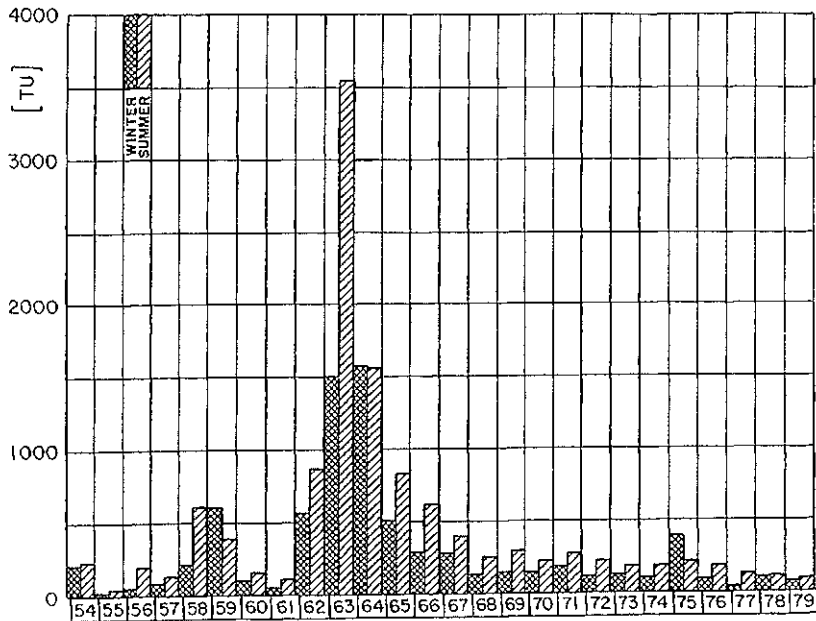


Fig. 1 Tritium concentrations in precipitation in central Europe, averages for the winter and summer half years.

meltwater and older groundwater in the runoff can be evaluated by the following balance equation:

$$c_t = dc_d + sc_s = c_d(1 - s) + c_s s \tag{2}$$

where:

d = proportion of the direct meltwater runoff in the total runoff;

s = proportion of the indirect runoff from groundwater reserves ($d + s = 1$);

c_t, c_d, c_s are tritium concentrations in the total runoff, meltwater runoff, and groundwater runoff.

Recalling Equation (1), the proportion of the indirect flow is analogous to the recession coefficient k which determines the proportion of the recession flow. Figure 2

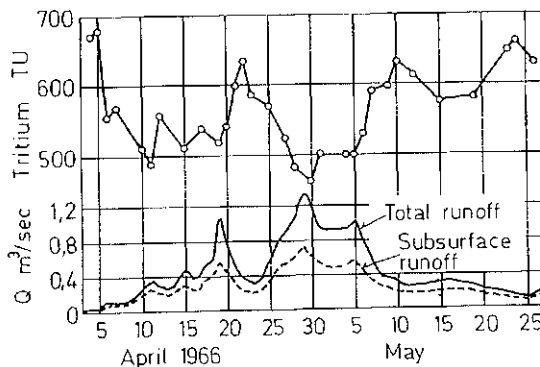


Fig. 2 Participation of indirect (groundwater) runoff in the total runoff of the basin Modry Dul, computed from tritium concentrations in the snow cover, groundwater and river flow (Dinçer *et al.*, 1970).

shows the runoff in the Modry Dul basin and the participating indirect flow computed by equation (2). The surprisingly high proportion of indirect flow, even in the peaks, suggests a revision of the traditional theory of streamflow generation outlined by Horton (1933). The new concept was confirmed in the Dischma basin (Martinec *et al.*, 1974, 1982a,b; Martinec, 1985) as well as in other basins (Sklash & Farvolden, 1979; Kobayashi, 1985) and, using deuterium and oxygen-18 as tracers, by Herrmann *et al.* (1979) and Rodhe (1981). For the development of SRM, it is important to note that the proportion of the indirect flow continuously decreases when the discharge increases and *vice versa*. Accordingly, the tentative step-wise adjustment of the recession coefficient adopted for the runoff simulation by Dinçer *et al.* (1970) was replaced by the following formula:

$$k_{n+1} = x \cdot Q_n^{-y} \quad (3)$$

where:

k = recession coefficient,

Q = discharge ($\text{m}^3 \text{s}^{-1}$),

x, y are constants which must be determined for the given basin by analysing runoff data;

$n, n + 1$ refer to the sequence of days.

In day-to-day runoff computations, the current runoff Q_n serves for computing k_{n+1} which determines the proportion of the immediate (within 24 h) and recession flow on the next day. The proportion of the recession flow thus computed does not exactly correspond to the proportion of indirect flow evaluated from tritium tracing (Martinec, 1975):

	Modry Dul, 2.65 km ² season 1966	Dischma, 43.3 km ² season 1973
Recession flow computed by k	56.5%	71.2%
Indirect flow from tritium data	62.6%	64.1%

In Modry Dul, $k < s$ which indicates that the direct flow finishes before the end of each 24 h period so that the actual proportion of the indirect flow is greater than that of the

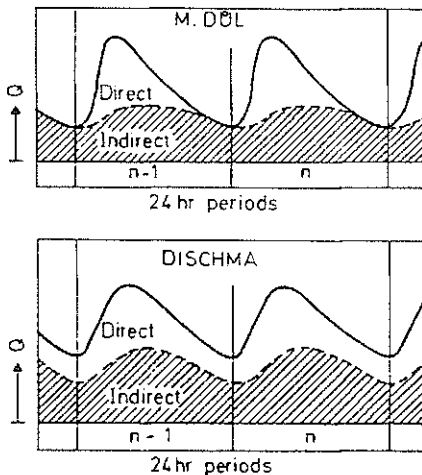


Fig. 3 Separation of the direct and indirect flow in the basins Modry Dul (2.65 km²) and Dischma (43.3 km²) based on tritium data.

computed recession flow. In Dischma, $k > s$ which means that the proportion of the indirect flow is smaller than that of the computed recession flow, probably because the direct flow is not completely finished at the end of the 24 h period. Figure 3 illustrates these conditions hypothetically. In spite of these discrepancies, the analogy between the recession flow and indirect flow (i.e. groundwater flow) helped to recognize that the recession coefficient is continuously changing in relation to the changing runoff. Another result of the tracer studies is the quick reaction of the indirect flow to fluctuations of the direct flow which is also evident from Fig. 2. In view of small velocities of water particles below the surface, this response can be only explained by assuming that infiltration quickly activates the outflow from groundwater storage into river channels. A study of this phenomenon was carried out in laboratory conditions on a small scale model (Stauffer & Dracos, 1984).

These findings are used in SRM for a simple and transparent transformation of input into the basin output (runoff) according to equations (1) and (3). In this way,

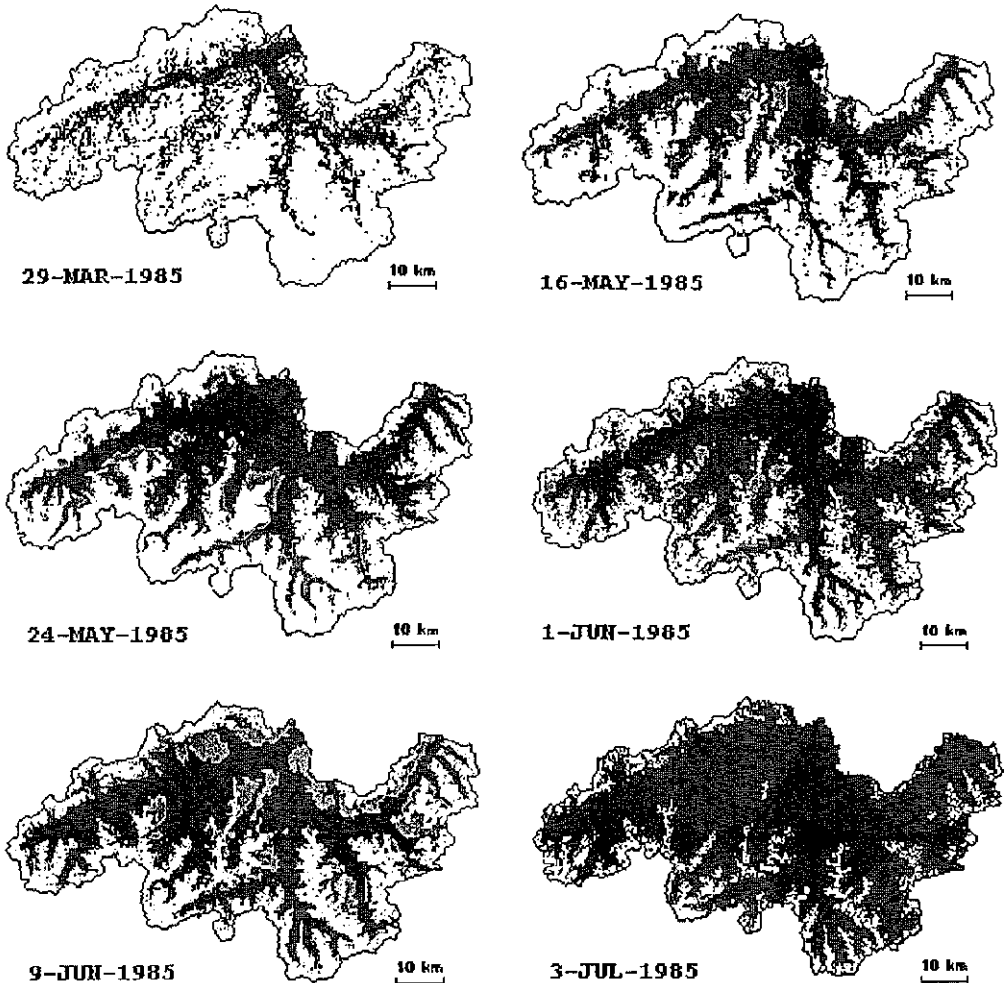


Fig. 4 Sequence of the snow cover maps from Landsat MSS 5 in the basin of the upper Rhine at Felsberg (3250 km^2) (Baumgartner, 1987).

complications could be avoided such as computing the velocity of overland flow or modelling the groundwater flow by a system of reservoirs.

REMOTE SENSING OF SNOW COVERED AREAS

The deterministic approach of the SRM model requires accurate measurements of the snow coverage which gradually decreases during the snowmelt season. Without remote sensing, the use of SRM would have been limited to small experimental basins. Thanks to the efficient snow cover mapping by satellites, it has been applied so far in 80 mountain basins situated in 25 different countries (Martinec *et al.*, 1998). As an example, Fig. 4 shows the gradual disappearance of the seasonal snow cover in the basin of the upper Rhine at Felsberg (3250 km², 560–3614 m a.s.l.) (Baumgartner, 1987). Characteristics of satellites suitable for snow cover mapping in the visible range are listed in Table 1.

The accuracy of snow cover mapping depends, of course, on the spatial resolution of sensors. The other aspect is the repeat period because daily snow covered areas required by the model must be interpolated from periodical satellite overflights. For basins with an elevation range exceeding 500 m, the depletion curves of the snow coverage must be derived for the respective elevation zones as shown in Fig. 5. These curves were interpolated from the sequence of snow cover maps shown in Fig. 4. In view of the frequent interference of clouds, satellites with a short repeat period (like NOAA-AVHRR) have a better chance to provide an adequate number of unobscured images during the snowmelt season than Landsat-type satellites which have a better spatial resolution but a repeat period of 2–3 weeks. Current efforts in remote sensing aim at solving this problem in several ways:

- (a) Development of methods to extrapolate the snow coverage from cloud-free areas of a basin to areas of a basin partially obscured by clouds (Ehrler *et al.*, 1997).
- (b) Improved interpretation of NOAA-AVHRR data by evaluating the snow coverage within each 1 km² pixel (Gomez-Landesia, 1997).
- (c) Improvement of the spatial resolution of sensors for satellites with a short repeat period (Hall *et al.*, 1995).
- (d) Development of methods of snow cover mapping by microwaves for all-weather monitoring of snow cover (Nagler & Rott, 1997).

Table 1 Satellites for snow cover mapping in the visible range.

Platform Sensor	Spatial resolution	Minimum size of area	Repeat period
Landsat			16–18 days
MSS	80 m	10–20 km ²	
TM	30 m	2.5–5 km ²	
NOAA AVHRR	1.1 km	100–500 km ²	12 hr
Meteosat			30 min
Visible	2.5 km	500–1000 km ²	
SPOT	10–20 m	2–3 km ²	26 days
MOS	50 m	5–10 km ²	17 days

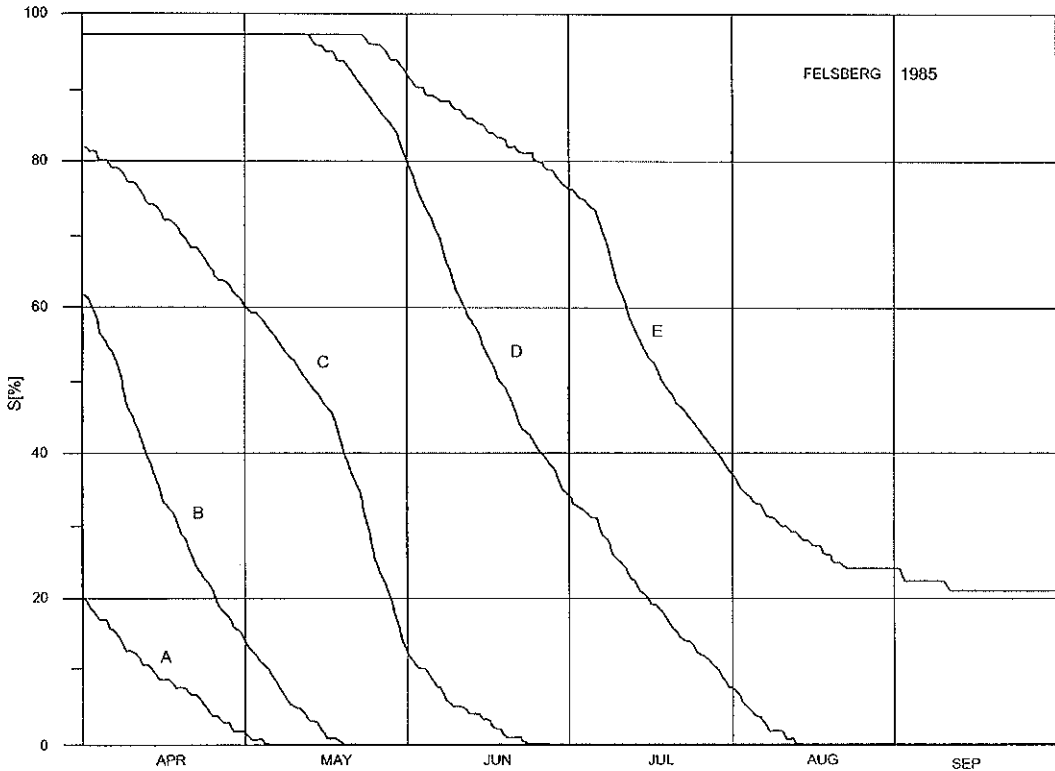


Fig. 5 Depletion curves of the snow coverage for five elevation zones of the Rhine-Felsberg basin, derived from the imagery in Fig. 4. A: 560–1100 m a.s.l., B: 1100–1600 m a.s.l., C: 1600–2100 m a.s.l., D: 2100–2600 m a.s.l., E: 2600–3600 m a.s.l.

RUNOFF COMPONENTS AND YEAR-ROUND RUNOFF MODELLING

In the course of years, the SRM model was adapted to conditions in large basins with a great elevation range, and convenient computer programs have been developed (Martinec *et al.*, 1998). However, the basic principles formulated in equations (1) and (3) remain the same. Thanks to the relative simplicity and transparent structure of the model, it is possible to extract intermediate information on the respective components contributing to runoff:

Seasonal snow cover: $a \cdot T \cdot S$

New snow during the snowmelt period: $a \cdot T(1 - S)$

Rain (liquid precipitation according to a critical temperature)

where:

a = the degree-day factor ($\text{cm} \cdot ^\circ\text{C}^{-1} \cdot \text{day}^{-1}$),

T = number of degree-day ($^\circ\text{C} \cdot \text{day}$),

S = snow covered area relative to total area.

Figure 6 shows the cumulative volumes of these components in three elevation zones of the Dischma representative basin (Martinec, 1975). The computed amounts are

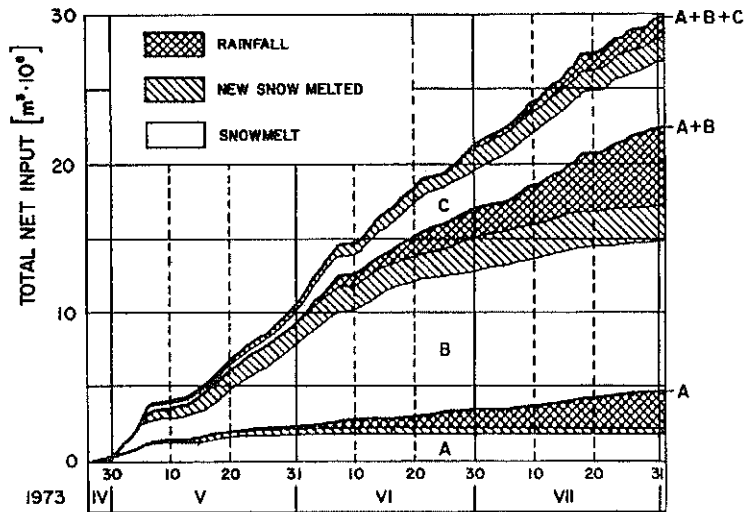


Fig. 6 Proportions of runoff components in the net input into the Dischma basin in the form of cumulative volumes for the elevation zones A, B, C.

already reduced by runoff coefficients taking into account the losses. Due to its larger area (24.5 km²), the contribution of zone B (2100–2600 m a.s.l.) is larger than that of zone A (8.9 km², 1668–2100 m a.s.l.) and C (9.9 km², 2100–3146 m a.s.l.). The seasonal snow cover is the largest contributor in the zones B and C, but in the low zone A it is rain. The contribution of new snow is relatively small except in the high zone C. It should be noted that this contribution refers to the snow-free area (1 - S) while new snow falling on the snowpack is integrated into the seasonal snow cover. In a tracer study distinguishing these three components, it would be necessary to compute the new snow contribution from the whole area and to decrease the contribution of the seasonal snow cover by the integrated amount of new snow.

CONCLUSION

An extensive tracer study of the snowmelt runoff process with the use of tritium, oxygen-18 and deuterium, revealed the need to revise the conventional runoff concept in snowmelt runoff basins, in particular the role of groundwater and of the recession flow. Using this knowledge, a snowmelt runoff model was designed which, at the same time, exploits progress in remote sensing because the computation is based on periodical satellite snow cover mapping. The SRM model may thus be regarded as the result of combining tracer analysis and remote sensing methodologies.

REFERENCES

- Baumgartner, M. E. (1987) Schneeschmelz—Abflusssimulationen basierend auf Schneeflächen-Bestimmungen mit digitalen Landsat-MSS und NOAA-AVHRR Daten (Snowmelt runoff simulations). *Remote Sensing Series* 11. Dept Geography, University of Zurich, Switzerland.
- Dinçer, T., Payne, B. R., Florkowski, T., Martinec, J. & Tongiorgi, E. (1970) Snowmelt runoff from measurements of tritium and oxygen-18. *Wat. Resour. Res.* 6(1), 110–124.

- Ehrler, C., Seidel, K. & Martinec, J. (1997) Advanced analysis of the snow cover based on satellite remote sensing for the assessment of water resources. In: *Remote Sensing and Geographic Information Systems for Design and Operation of Water Resources Systems* (ed. by M. F. Baumgartner, Gert A. Schultz & A. I. Johnson) (Proc. Rabat Symp., April–May 1997), 83–91. IAHS Publ. no. 242.
- Gomez-Landesa, E. (1997) Evaluacion de recursos de agua en forma de nieve mediante teledeteccion usando satelites de la sene NOAA (Evaluation of water resources in the form of snow by remote sensing using NOAA satellites). PhD Thesis, Universidad Politenica de Madrid, Madrid, Spain.
- Hall, D. K., Riggs, G. A. & Salomonson, V. V. (1995) Development of methods for mapping global snow cover using moderate resolution imaging spectroradiometer data. *Remote Sens. Environ.* **54**, 127–140.
- Herrmann, A., Martinec, J. & Stichler, W. (1979) Study of snowmelt runoff components using isotope measurements. In: *Proceedings of a Meeting on Modeling of Snow Cover Runoff*, 288–296. Cold Regions Research and Engineering Laboratory, Hanover, USA.
- Horton, R. E. (1933) The role of infiltration in the hydrological cycle. *Trans. AGU* **14**, 446–460.
- Kobayashi, D. (1985) Separation of the snowmelt hydrograph by stream temperatures. *J. Hydrol.* **76**, 155–162.
- Martinec, J. (1975) New methods in snowmelt–runoff studies in representative basins. In: *The Hydrological Characteristics of River Basins* (Proc. Tokyo Symp., December 1975), 99–107. IAHS Publ. no. 117.
- Martinec, J. (1985) Time in hydrology. In: *Facets of Hydrology* (ed. by J. C. Rodda), vol. II, 249–290. John Wiley, London.
- Martinec, J., Oeschger, H., Schotterer, U. & Siegenthaler, U. (1982a) Snowmelt and groundwater storage in an Alpine basin. In: *Hydrological Aspects of Alpine and High Mountain Areas* (ed. by J. W. Glen) (Proc. Exeter Symp., July 1982), 169–175. IAHS Publ. no. 138.
- Martinec, J., Schotterer, U. & Siegenthaler, U. (1982b) Bestimmung des Grundwasseranteils im Schnee- und Regenabfluss im Schweizerischen Einzugsgebiet Dischma (Determining the proportion of groundwater in the snowmelt- and rainfall runoff in the Swiss basin of Dischma) (in German with English abstract). In: *Proceedings 4th SUWT International Symposium on Tracer Techniques in Hydrology* (ed. by C. Leibundgut & R. Weingartner). *Beitraege zur Geologie der Schweiz-Hydrologie*, no. 28, part II, 459–470. Bern.
- Martinec, J., Rango, A. & Roberts, R. (1998) Snowmelt runoff model (SRM) user's manual. *Geographica Bernensia*, P 35, Dept Geography, Univ. Bern.
- Martinec, J., Siegenthaler, U., Oeschger, H. & Tongiorgi, E. (1974) New insights into the runoff mechanism by environmental isotopes. In: *Proceedings Symposium on Isotope Techniques in Groundwater Hydrology*, vol. 1, 129–143. International Atomic Energy Agency, Vienna.
- Nagler, T. & Rott, H. (1997) The application of ERS-1 SAR for snowmelt runoff modelling. In: *Remote Sensing and Geographic Information Systems for Design and Operation of Water Resources Systems* (ed. by M. F. Baumgartner, Gert A. Schultz & A. I. Johnson) (Proc. Rabat Symp., April–May 1997), 83–91. IAHS Publ. no. 242.
- Rango, A. & Itten, K. L. (1976) Satellite potentials in snowcover monitoring and runoff prediction. *Nordic Hydrol.* **7**, 209–230.
- Rodhe, A. (1981) Spring flood, meltwater or groundwater. *Nordic Hydrol.* **12**, 21–30.
- Seidel, K., Ehrler, C. & Martinec, J. (1996) Multisensor analysis of satellite images for regional snow distribution. In: *Progress in Environmental Research and Applications* (Proc. 15th EARSeL Symp., Basel, Switzerland), 213–220. A. A. Balkema, Rotterdam/Brookfield.
- Sklash, M. G. & Farvolden, R. N. (1979) The role of groundwater in storm runoff. *J. Hydrol.* **43**, 43–65.
- Stauffer, F. & Dracos, T. (1984) Local infiltration into layered soil and response of the water table, experiment and simulation. In: *Frontiers of Hydrology*, 228–245. WRP, Littleton, Colorado, USA.